Eur. Phys. J. B **47**, 167–170 (2005)
DOI: 10.1140/epjb/e2005-00323-0

THE EUROPEAN PHYSICAL JOURNAL B

Electronic properties of intersubband transition in (CdS/ZnSe)/BeTe quantum wells

S. Abdi-Ben Nasrallah[a], N. Sfina, and M. Said

Unité de Recherche de Physique des Solides, Département de Physique, Faculté des Sciences de Monastir, 5019 Monastir, Tunisia

Received 4 April 2005
Published online 11 October 2005 –

Abstract. In view of the fact that the bandwidth required in optical fiber communication systems will exceed 100 Gb s^{-1}, ultrafast optical switching and modulation devices with high efficiency must be developed. Given that intersubband transitions (ISBT) in quantum wells (QWs) are one of the important ultrafast phenomena, a numerical study of intersubband transition (ISBT) properties in (CdS/ZnSe)/BeTe QWs is considered. The structure modeled consists of a few monolayers of CdS embedded in a ZnSe/BeTe QW. A self-consistent analysis is made to achieve the desired properties and device applications. Variation of CdS well thickness leads to tailoring of the band alignment, achieving optical transitions in the wavelength range of 1.33–1.55 μm wavelengths for applications in optical fiber transmission. To analyze the optical behavior of the heterostructure under investigation, we have calculated the CdS well thickness-dependant oscillator strengths and electron emission energy of the intersubband transition between the two first states in the well. An attempt to explain our results will be presented.

PACS. 81.05.Dz II-VI semiconductors – 85.35.Be Quantum well devices (quantum dots, quantum wires, etc.) – 42.81.Wg Other fiber-optical devices – 42.65.Re Ultrafast processes; optical pulse generation and pulse compression

1 Introduction

With the advent of modern epitaxial growth techniques such as molecular beam epitaxy (MBE), it has become possible to grow semiconductor superlattices and quantum well structures and tailor the band structures to achieve the desired properties for device applications. Intersubband transitions (ISBT) in quantum wells (QWs) are very important both from a fundamental physics perspective and for device applications. Due to its fast relaxation process which is one of its technological advantages, the ISBT is involved in several optoelectronic devices such as quantum cascade lasers [1], infrared detectors [2] and optical modulators [3]. In order to take advantage of the fast relaxation time for applications in the optical fiber transmission window around $\lambda \sim 1.55$ μm, ISB transition with high energy is required, so the use of materials with large conduction band offset is needed. Many attempts have been made to shorten the ISB transition wavelength. Smet et al. [4] have used InGaAs/AlAs QW while Gmachi et al. [5] have considered a GaN/AlGaN heterostructure. For the same reason, Akimoto et al. [6] proposed a ZnSe/BeTe based structure showing an ISBT around 1.6 μm. The ZnSe/BeTe system displays features in structure and banding similar to those of III–V semiconductor compounds. It was developed a few years ago in an attempt to get better lifetime in II–VI optoelectronic devices by means of BeTe and to improve the reliability of ZnSe based devices. The ZnSe/BeTe QW is important for ISBT switches due to its very large conduction band discontinuity of 2.3 eV [7]. Moreover, the higher ionicity of ZnSe leads to an ultra fast carrier relaxation in ZnSe/BeTe QW comparable to that of III–V Nitrides. However, the use of ultrafast pulses requires that the optical pulse occupies an extremely short distance in space and this means that the overall optical device and circuit is very compact. Nevertheless, the quantum confinement effects in a thin ZnSe QW can raise the Γ conduction-band state of the well (level E_2 in Fig. 3a) above the conduction-band state X of the BeTe barrier (state E_1' in Fig. 3a) leading to an indirect band-gap configuration with a slow relaxation time. This generates a carrier relaxation in two steps: $E_2 \rightarrow E_1'$ then $E_1' \rightarrow E_1$. In this case, the carrier dynamics is controlled by a slow relaxation to the Γ state. This affects negatively the overall relaxation time and the ISBT is not detected [8]. To surmount this difficulty and ensure the ISBT in this structure, we have inserted into the middle of the thin ZnSe well a CdS layer.

In the following, and after a brief description of the calculation method, we present in section three modeling

[a] e-mail: samiaabdi@myway.com

of the proposed (CdS/ZnSe)/BeTe structure. With the intention of achieving the ISBT $E_1 \rightarrow E_2$ with wavelengths in the range of 1.33−1.55 μm essential for optical fiber communication systems, the thickness L_w of CdS QW is treated as a parameter.

2 Computational methods

The modelled heterostructure consists of a CdS well embedded into two 0.6 nm ZnSe layers. This region is n-doped and limited by thin BeTe barriers; the whole is surrounded by two 7.5 nm ZnSe layers as spacers. This system combines advantages of both high n-dopability in the CdS/ZnSe and high conduction-band offset at ZnSe/BeTe ($\Delta E_c = 2.3$ eV). The electronic states of this system can be obtained using the effective mass theory and the local density approximation [9]. In the one band version of the envelope function approximation, the quantized energy levels E_ν for subbands ν and their related wave functions Φ_ν can be achieved by the self-consistent solution of the one-dimensional Schrödinger and Poisson equations.

In the Schrödinger equation:

$$\left[\frac{-\hbar^2}{2}\frac{d}{dz}\frac{1}{m^*(z)}\frac{d}{dz} + V_H(z) + V_{\mathrm{XC}}(z) + V_B(z) - E_\nu\right]\phi_\nu(z) = 0 \quad (1)$$

z is the growth direction, $\hbar$ is the Planck's constant, $m^*(z)$ is the electron effective mass, ν is the subband index, $V_H(z)$ is the Hartree potential energy which is determined by the Poisson equation:

$$\varepsilon_0\frac{d}{dz}\left[\varepsilon_r(z)\frac{d}{dz}V_H(z)\right] = e^2\left[N_D(z) - n(z)\right] \quad (2)$$

$V_B(z)$ is the potential energy due to the heterojunction-band-edge discontinuities and $V_{\mathrm{XC}}(z)$ is the exchange-correlation potential whose expression was taken from reference [10]

$$V_{\mathrm{XC}}(z) = -0.916\frac{e^2}{6\pi\varepsilon_0\varepsilon_r(z)}\left[\frac{3n(z)}{4\pi}\right]^{1/3}$$

where $N_D(z)$ is the total density of donor atoms in ZnSe and CdS layers and $\varepsilon_r(z)$ is the relative dielectric constant. Note that $n(z)$ is the local density of confined electrons established by the equation:

$$n(z) = \sum_\nu n_\nu \left|\Phi_{\nu,k_z}(z)\right|^2$$

with n_ν the density of electrons for the subband ν deduced by the relation:

$$n_\nu = \frac{m^* k_B T}{\pi\hbar^2}\mathrm{Ln}\left[1 + \exp\frac{E_F - E_\nu}{k_B T}\right]$$

where E_F is the Fermi level verifying the following equation:

$$N_D L_d = \sum_\nu n_\nu$$

with L_d the thickness of the doped zone. Numerically, the problem was treated using the finite differential method.

To achieve our calculation, values of the direct Γ band gaps $E_{\mathrm{g},\Gamma}(\mathrm{ZnSe}) = 2.82$ eV and $E_{\mathrm{g},\Gamma}(\mathrm{BeTe}) = 4.53$ eV [11] are used. For band gaps associated with the X valley we have used $E_{\mathrm{g,X}}(\mathrm{ZnSe}) = 4.54$ eV and $E_{\mathrm{g,X}}(\mathrm{BeTe}) = 2.6$ eV [11]. For the electron effective masses we have used $m^*_{\mathrm{e},\Gamma}(\mathrm{ZnSe}) = 0.19$ [12], $m^*_{\mathrm{e},\Gamma}(\mathrm{BeTe}) = 0.19$ [12] and $m^*_{\mathrm{e},\Gamma}(\mathrm{CdS}) = 0.19$ [13], all masses are considered in unit m_0 with m_0 the free electron mass. Note that, because of its direct band gap nature, CdS has the same parameters whether the structure is cubic or hexagonal. The relative dielectric constant $\varepsilon_r(z)$ is equal to 5.4 for ZnSe [14], 4.5 for BeTe [12] and 5.5 for CdS [13]. The total density of donors in ZnSe and CdS layers $N_D(z)$ is taken equal to 1.5×10^{19} cm^{-3} and leads to highly n-type doped QWs.

3 Results and discussion

First, we have varied the ZnSe well width for ZnSe/BeTe QW ($\Delta E_c = 2.3$ eV) (Fig. 3a) in an attempt to achieve the ISBT with 1.55 μm. However, in above structure, achieving the ISBT and attaining the range of wavelengths essential in optical fiber communication systems are competitive processes. In fact, by decreasing the ZnSe well thickness sufficiently in order to drop the two Γ subbands E_1 and E_2 below the X one E'_1 so that the ISBT can appear, the emission energy (the separation between the E_1 and E_2 levels) $\Delta E = E_2 - E_1$ becomes much lower than 0.8 eV and the shortest ISBT wavelength due to an optical transition between the first and the second levels E_1 and E_2 is 2.4 μm. On the other hand, the ISBT can occur in the CdS/ZnSe QW [15] which interface band offset is $\Delta E_c = 0.8$ eV, but we can never reach an emission energy ΔE higher than 0.4 eV i.e. a wavelength shorter than 2.9 μm. Taking into account these considerations, we thought of using the CdS/BeTe QW. Unfortunately, a trial growth of such a structure has shown a degraded surface. Consequently, we have opted for the (CdS/ZnSe)/BeTe structure (Fig. 3b). ZnSe layer inserted between BeTe and CdS is important (imperative) since it enhances the interface smoothing and improves the structural quality of devices. It is essential to mention the importance of the BeTe barrier in the structure. In fact, for the (CdS/ZnSe)/BeTe QW, the energy of the first subband is situated below the ZnSe conduction band edge while this first level is located near the midgap state unexpectedly incorporated in the BeTe barrier for ZnSe/BeTe QW. R. Akimoto et al. [8] have explained that this midgap state in BeTe compensates the carrier in the well and avoids the ISBT with aimed range wavelengths in ZnSe/BeTe QW.

By varying the CdS QW thickness in our structure, we can tailor the band alignment achieving ISBT emission in this range. The results of numerical calculations for

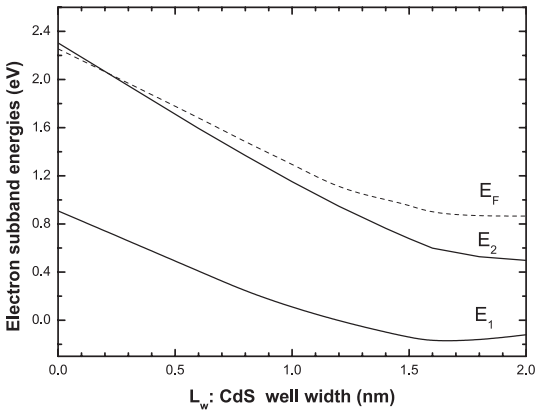

Fig. 1. Confinement energies of electron states E_1 and E_2 as well as Fermi level (eV) versus the CdS well width L_w (nm).

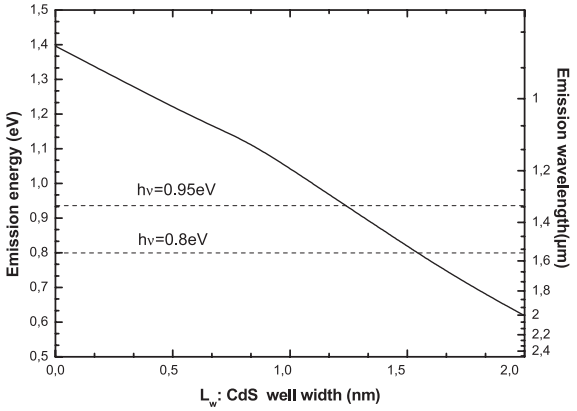

Fig. 2. The CdS well width-dependent emission energies and emission wavelengths achieving the transitions realizing optical fiber communication systems.

the energy electron levels E_1 and E_2 as well as the Fermi level versus the CdS well width are presented in Figure 1. The confinement energy decreases when L_w increases and as expected, larger confinement can be achieved in thin QWs. However, for very thin CdS wells (L_w lower than 0.2 nm), only the fundamental Γ subband of ZnSe is occupied by electrons. For a larger CdS well, the first excited Γ subband of ZnSe is more and more populated. The decrease of E_1 and E_2 levels makes them lower than the conduction-band state X of the BeTe barrier and the fast direct ISBT $\Gamma - \Gamma$ involving E_1 and E_2 wave functions occurs indicating that the Γ(ZnSe)–X(BeTe) electron transfer is suppressed. To investigate this ISBT, the CdS well width-dependent emission energy and emission wavelengths λ are calculated. As can be seen in Figure 2, the emission energy decays from 1.4 eV without the CdS well to 0.6 eV (0.83 to 2 μm) covering the optical fibre communication wavelengths (1.33 $\rightarrow$ 1.55 μm). To make use of this wavelength range, the CdS layer thickness increases from 1.20 to 1.54 nm. The scheme potential of this design for 1.55 μm (0.8 eV) wavelength emission is shown in Figure 3. Figure 3a illustrates the band line-up in ZnSe/BeTe QW for conduction band states Γ and X (solid line and dotted line respectively). In such a structure, relaxation to X valley (state E_1') and subsequent acoustic phonon relaxation to the E_1 state is a process competitive with direct $\Gamma - \Gamma$ one. In Figure 3b, the CdS QW implanted in ZnSe one make Γ levels E_1 and E_2 lower than X state. The fast direct relaxation $\Gamma - \Gamma$ decay is the predominant relaxation process.

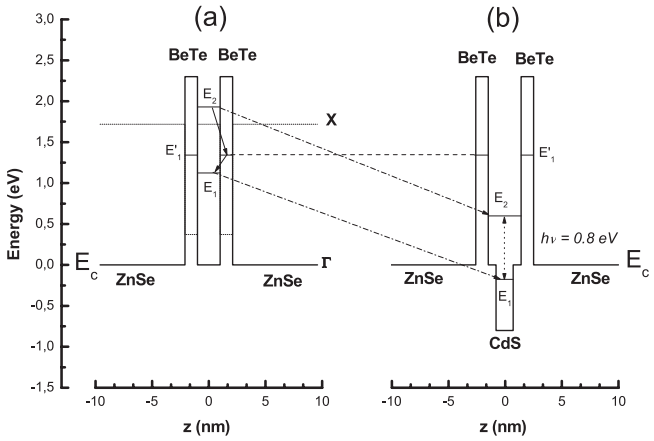

Fig. 3. Schematic of band alignment a) ZnSe/BeTe and b) (CdS/ZnSe)/BeTe quantum wells. The introduction of a CdS layer in ZnSe/BeTe heterostructure can eliminate the slow carrier relaxation process of Γ(ZnSe)–X(BeTe) transfer which is observed in ZnSe/BeTe QW (a). Strong ISB transition at the wavelength of 1.55 μm ($\Delta E = 0.8$ eV) is shown.

To study and carry out the quantum efficiency of our design, we have calculated the oscillator strength of the transition which is defined by the expression [16]

$$f_{l\rightarrow k} = \frac{2m_0}{\hbar^2}(E_l - E_k)\,|\langle\phi_l\,|z|\,\phi_k\rangle|^2$$

where $(E_l - E_k)$ is the energy difference between the initial and finite states and $|\langle\phi_l\,|z|\,\phi_k\rangle|$ is the dipole matrix element of the transition. In Figure 4, we have represented the emission wavelengths λ and the oscillator strengths for ISBT $f_{e1\rightarrow e2}$ versus the CdS well width for two BeTe barrier thicknesses. As can be seen, $f_{e1\rightarrow e2}$ decreases as L_w increases. But it is shown that this decrease is not significant and the transition oscillator strengths remain relatively high. This means that the efficiency of radiative recombination in active material of (CdS/ZnSe)/BeTe heterostructure is highly preserved (2.707×10^3 and 1.976×10^3 respectively for 1.55 and 1.33 μm) and the quantum efficiency of luminescence is good. For the desired emission wavelength, we can obtain from the figure the optimum parameters of the modelled design. For wavelengths solicited in optical communication and covering the range (1.33 $\rightarrow$ 1.55 μm), thicknesses values between (1.2−1.6) nm and (1.2−1.5) nm are needed respectively for CdS well and BeTe barrier. In Figure 5, the conduction band, electron energy levels E_1 and E_2 with their related wavefunctions for our modeled device with $\lambda = 1.55$ μm ($\Delta E = 0.8$ eV) are represented.

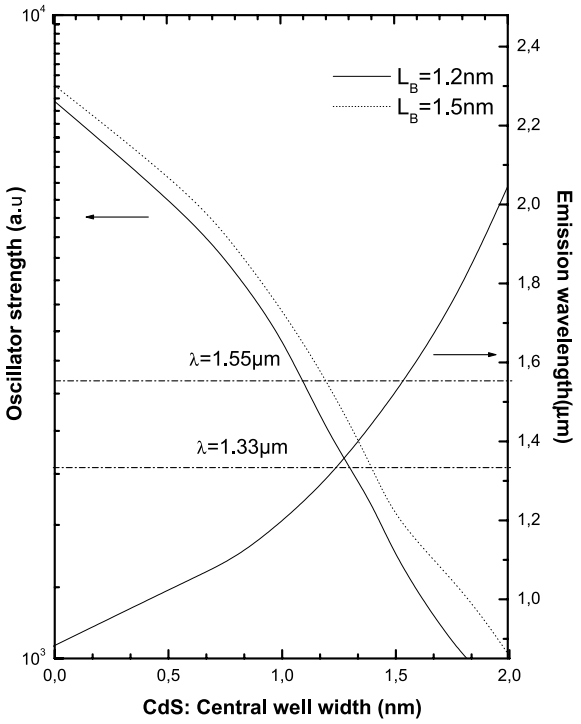

Fig. 4. The oscillator strength (for two BeTe barrier widths L_B) and the wavelength λ (μm) versus CdS well width L_w for intersubband transition $E_1 \rightarrow E_2$.

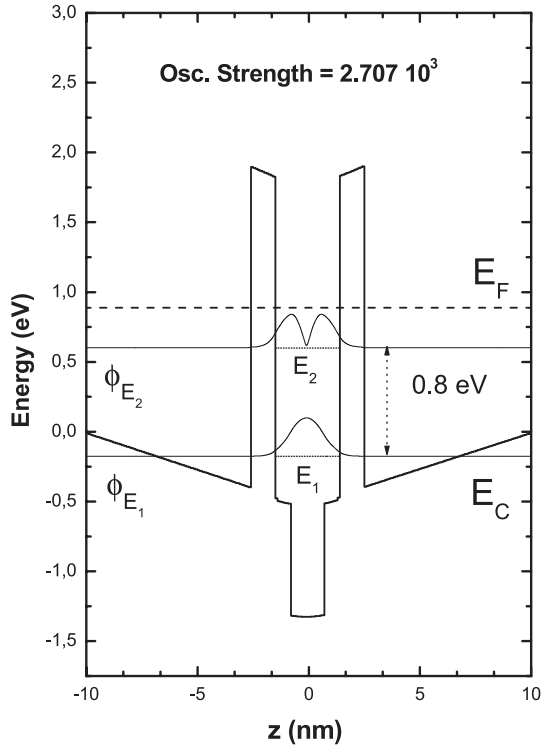

Fig. 5. Band structure and wave functions of the two first states for modeled (CdS/ZnSe)/BeTe QW.

4 Conclusion

With a view to possible device applications such as ultrafast all optical switches and modulators, our attention has been devoted to the fibre optic emissions (1.33 $\rightarrow$ 1.55 μm). We have presented a model of ISBT of carriers in n-type doped (CdS/ZnSe)/BeTe QWs. The introduction of a thin CdS layer in the ZnSe/BeTe heterostructure can avoid the slow carrier relaxation process of Γ(ZnSe)–X(BeTe) transfer which has been observed in ZnSe/BeTe QW. Strong ISBT has been demonstrated between the two lowest confined electron states. We have treated the CdS well thickness as a parameter to achieve designs for desired applications. The optimum parameters (CdS well width $L_w = 1.54$ nm and BeTe barrier thickness $L_B = 1.2$ nm) lead to 1.55 μm light emission with good quantum efficiency.

References

1. See J. Faist, F. Capasso, D. Sivco, C Sirtori, A.L. Hutchinson, S.N.G. Chu, A.Y. Cho, Science **264**, 553 (1994)
2. B.F. Levine, R.J. Malik, J. Walker, K.K. Choi, C.G. Bethea, D.A. Kleinman, M. Vanderberg, Appl. Phys. Lett. **50**, 273 (1987)
3. *Intersubband Transitions in Quantum Wells: Physics and Devices*, edited by S.S. Li, Y.-K. Su (Kluwer Academic, Dodrecht, 1998)
4. J.H. Smet, L.H. Peng, Y. Hirayama, C.G. Fonstad, Appl. Phys. Lett. **64**, 986 (1994)
5. C. Gmachi, S.V. Frolov, H.M. Ng, S.-N.G. Chu, A.Y. Cho, Electron. Lett. **37**, 378 (2001)
6. R. Akimoto, Y. Kinpara, K. Akita, F. Sasaki, S. Kobayashi, Appl. Phys. Lett. **78**, 580 (2001)
7. A. Waag, F. Fisher, H.-J. Lugauer, Th. Liz, U. Zehnder, W. Ossau. T. Gerhardt, M. Möller, G. Landweher, J. Appl. Phys. **80**, 792 (1996)
8. R. Akimoto, K. Akita, F. Sasaki, T. Hasama, Appl. Phys. Lett. **81**, 2998 (2003)
9. F. Ben Zid, A. Bhouri, H. Mejri, R. Tlili, M. Said, J. Appl. Phys. **91**, 9176 (2002)
10. P. Ruden, G.H. Dohler, Phys. Rev. B **27**, 3538 (1983)
11. A.A. Toporov, O.V. Nekrutkina, M.O. Nestoklon, S.V. Sorokin, D.D. Solnyshkov, S.V. Ivanov, A. Waag, G. Landwehr, Phys. Rev. B **67**, 113307 (2003)
12. S. Abdi-Ben Nasrallah, S. Ben Afia, H. Belmabrouk, M. Said, Eur. Phys. J. B **43**, 3 (2005)
13. M.V. Rama, J. Chem. Phy. **95**, 8309 (1991)
14. O. Madelung, *Semiconductors Basic Data*, 2nd revised edn. (Springer, 1996)
15. M. Göppert, R. Becker, S. Petillon, M. Grün, C. Maier, A. Dinger, C. Kligshirn, J. Cryst. Growth **214/215**, 625 (2000)
16. W.Q. Chen, T.G. Andersson, J. Appl. Phys. **73**, 4484 (1993)